Inorganic Chemistry

Article

pubs.acs.org/IC

$PbMnIn_2S_5$: Synthesis, Structure, and Properties

Peng Yu,[†,‡] Li-Ming Wu,[†] and Ling Chen*[,†]

[†]Key Laboratory of Optoelectronic Materials Chemistry and Physics, Fujian Institute of Research on the Structure of Matter, Chinese Academy of Sciences, Fuzhou, Fujian 350002, People's Republic of China

[‡]Graduate University of the Chinese Academy of Sciences, Beijing 100039, People's Republic of China

Supporting Information

ABSTRACT: The first manganese member in a Pb−M−In−Q system, $PbMnIn_2S_5$, has been discovered by a high-temperature solid-state reaction. It adopts a $Sr_2Tl_2O_5$ structure type in orthorhombic space group *Cmcm* (No. 63) with a = 3.896(2) Å, b = 12.731(7) Å, c = 15.770(9) Å, and Z = 1. The structure consists of corrugated layers made by $(In1/Mn1)S_6$ octahedra that are further interconnected by chains of edge-sharing $(In2/Mn2)S_6$ octahedra into a three-dimensional framework; Pb^{2+} cations are coordinated in PbS_8 bicapped triangular prisms that are face-shared along the a direction. The crystallographically distinguished octahedrally coordinated 8*f* and 4*b* sites are disordered by Mn and In atoms. Such a structure allows antiferromagnetic interactions between the high-spin Mn^{2+} anions. The optical band gap is measured to be about 1.45 eV.

INTRODUCTION

Transition-metal chalcogenides have been intensively studied because of their structural flexibility and interesting physical properties.[1−3] Among them, quaternary Pb−M−In (Sb)−Q chalcogenides, where M = transition metal and Q = S and Se, are a recent hot topic because of their unusual magnetic properties. In 2003, an interesting one-dimensional Heisenberg antiferromagnetic $[FeS_6]$ chain in $Pb_4FeSb_6S_{14}$ was discovered to exhibit a short-range magnetic ordering below 33.5 K.[4] After that, Fe atoms were observed in 2006 to partially substitute Pb (or In) octahedral sites in ferromagnetic $Pb_{8.04}Fe_{0.47}In_{17.37}Se_{34}$[5] or antiferromagnetic $Pb_{5.5}Fe_{1.5}In_{10}S_{22}$.[6] In 2010, Fe-atom substitution in $Pb_4Sb_4Se_{10}$[7] generated $Pb_{0.75}Fe_{3.25}Sb_4Se_{10}$ and $Pb_3FeSb_4Se_{10}$, which contain unique ferromagnetic chains of dimeric $[Fe_2Se_{10}]$.[8] Interestingly, some of such compounds illustrate that the substitution of a transition metal at Pb or In (Sb) sites may generate low-dimensional magnetic domains that are embedded in the original structures and give rise to attractive magnetic properties. Obviously, the structural roles of transition metals in such systems are also important regarding the stabilization and formation of new compounds.

In this paper, we report the first manganese member in a Pb−M−In−Q system, $PbMnIn_2S_5$, adopting a $Sr_2Tl_2O_5$ structure type that is observed for the first time in such systems. The title compound enriches the structural diversity of the $AM_xPn_{3-x}Q_5$ family (A = univalent and divalent cations; M = transition metal, Pn = Sb, Bi, As, and In; Q = S, Se, and Te; $0 \le x < 3$).[9−14] The synthesis, single-crystal structure, optical band gap, and magnetic properties were reported.

EXPERIMENTAL SECTION

Synthesis. All of the operations were completed in an argon-filled glovebox with controlled oxygen and moisture levels below 0.1 ppm. Pb (99.9%), In (99.99%), and S (99.999%) were purchased from Alfa Aesar China (Tianjin) Co., Ltd., and Mn (99.99%) was purchased from ABCR GmbH & Co. KG. All of the reactions were completed in evacuated fused-silicon tubes (under a 10^{-3} Pa atmosphere) in a resistance furnace with controlled temperature. The single crystals of $PbMnIn_2S_5$ were obtained from the reaction of a Pb, Mn, In, and S elemental mixture of a loading mole ratio of 3:3:5:14 and a total weight of about 300 mg. The reaction was heated to 1100 °C within 85 h, maintained for 70 h, and then cooled to 450 °C at 5 °C h^{-1} before the furnace was switched off. The product contained beautiful bar-shaped metallic silver crystals of $PbMnIn_2S_5$, together with byproducts of black PbS chunk, ternary $MnIn_2S_4$, and a trace of an unknown phase (Figure 1a). Many efforts had been made by adjusting the reaction temperature and loading ratio to get a pure phase of the title compound, but they unfortunately failed. Because of their distinguishable shapes and color, we were able to manually pick considerable numbers of crystals, and all properties reported here were measured on such crystals (Figure 1b).

Crystal Structure Determinations. A black bar-shaped crystal with approximate dimensions of 0.10 × 0.09 × 0.18 mm^3 mounted on the tip of a glass fiber was selected to collect data on a Mercury CCD automatic diffractometer equipped with graphite-monochromated Mo Kα radiation (λ = 0.71073 Å) at room temperature. The data were corrected for Lorentz factors, polarization, and absorption. Absorption correction based on a multiscan technique was performed by the *SADABS* program.[15,16] The space group was determined to be *Cmcm* (No. 63) based on systematic absences, *E*-value statistics, and subsequent successful refinements of the structure. The structure was solved by direct methods and refined by a full-matrix least-squares fitting on F^2 by *SHELX-97*.[17] There are three metal sites (M1, M2, and M3), where the M1 site is 8-fold-coordinated by S and the M2 and M3 sites are 6-fold-coordinated by S. The initial model with formula "$PbIn_3S_5$" ($R1$ = 0.0466, $wR2$ = 0.1634) was built with M1 assigned as Pb and M2 and M3 as In, according to their different radii, X-ray scattering properties, and atomic weights. Clearly, the empirical formula "$Pb^{2+}(In^{3+})_3(S^{2-})_5$" could not reach the charge balance. Thereby, the occupancies on M1, M2, and M3 that converged to $R1$ =

Received: August 25, 2012
Published: January 7, 2013

   dx.doi.org/10.1021/ic3018584 | *Inorg. Chem.* 2013, 52, 724−728

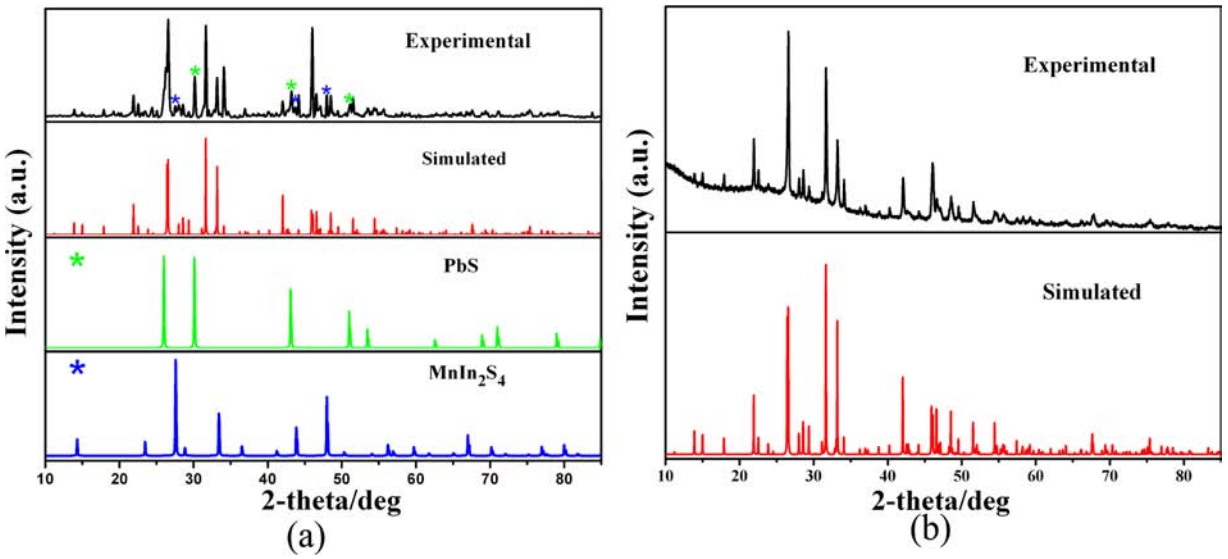

Figure 1. (a) Experimental and simulated XRD patterns of $PbMnIn_2S_5$. Stars indicate byproducts (PbS and $MnIn_2S_4$). (b) Experimental XRD pattern of handpicked $PbMnIn_2S_5$ crystals and its simulated pattern.

Table 1. Crystal Data and Structural Refinements for $PbMnIn_2S_5$

chemical formula	$PbMnIn_2S_5$
fw	652.13
cryst syst	orthorhombic
space group	*Cmcm* (No. 63)
cryst shape/color	bar/black
a (Å)	3.896(2)
b (Å)	12.731(7)
c (Å)	15.770(9)
V (Å^3)	782.2(7)
Z	1
temperature (K)	293(2)
ρ_{calcd} (g cm^{-3})	5.538
θ range (deg)	3.20–24.96
collected/unique reflns	2454/415
abs coeff (mm^{-1})	7.522
extinction coeff	0.0018(2)
$R1/wR2$ $[I > 2\sigma(I)]^a$	0.0215/0.0533
$R1/wR2$ (all data)	0.0215/0.0533
largest diff peak/hole (e Å^{-3})	1.924/−1.239
GOF on F_o^2	1.107

$^a R1 = \sum||F_o| - |F_c||/\sum|F_o|$ for $F_o^2 > 2\sigma(F_o^2)$; $wR2 = \sum[w(F_o^2 - F_c^2)]/\sum[w(F_o^2)^2]^{1/2}$, where $w = 1/[\sigma^2F_o^2 + (0.0275P)^2 + 9.9329P]$, and $P = (F_o^2 + 2F_c^2)/3$.

0.0315 and $wR2$ = 0.1005 were freely refined, after which the M1 occupancy did not change, while those of the M2 and M3 sites decreased and unbalanced formula "$Pb_4In_{10.2}S_{20}$" was converged. The isotropic displacement parameters (U_{eq}) for M2 (from 0.026 to 0.019 Å^2) and M3 (from 0.023 to 0.017 Å^2) decreased. Subsequently, considering that the existence of Mn revealed by energy-dispersive X-ray (EDX) measurement and the fact that the ionic radii of In^{3+} and Mn^{2+} (In^{3+}, 0.800 Å; Mn^{2+}, 0.830 Å) are similar, Mn was introduced into the M2 and M3 sites with mixed occupancies. The subsequent refinement generated In/Mn occupancies of 0.57/0.43 and 0.87/0.13 on M2 (8*f*) and M3 (4*b*) sites, which converged to a neutral formula "$PbMnIn_2S_5$", agreeing with the EDX result of $Pb_{0.90(6)}Mn_{0.90(8)}In_2S_{5.2(3)}$ and better R values of $R1$ = 0.0215 and $wR2$ = 0.0533. Crystallographic data and structural refinements for this compound are summarized in Table 1. Positional and equivalent isotropic displacement parameters and relevant bond distances are listed in Tables 2 and 3. In order to probe the possible phase width, five crystals from different batches were selected to collect the diffraction data (Table S1 in the Supporting Information); the successful refinement indicated that there is no phase width observed (Table S2 in the Supporting Information).

Table 3. Selected Interatomic Distances (Å) in $PbMnIn_2S_5$[a]

bond	length (Å)	bond	length (Å)
Pb−S1×2	2.755(3)	M1−S2×2	2.757(2)
Pb−S2×2	3.307(3)	M1−S3×2	2.592(2)
Pb−S3×4	3.182(2)	M2−S2×4	2.796(2)
M1−S1×1	2.511(2)	M2−S3×2	2.439(3)
M1−S2×1	2.670(3)		

[a] M1 and M2 are disordered by Mn and In atoms, as indicated in Table S2 in the SI.

Table 2. Atomic Positions, Occupancies, and Equivalent Isotropic Displacement Parameters for $PbMnIn_2S_5$

atom	Wyckoff site	*x*	*y*	*z*	occupancy	U_{eq} (Å^2)[a]
Pb	4*c*	$^1/_2$	0.44972(5)	$^1/_4$	1.0	0.0254(3)
M1 (In1/Mn1)	8*f*	0	0.21726(7)	0.39575(6)	0.57/0.43	0.0131(3)/0.0131(3)
M2 (In2/Mn2)	4*b*	1.0	$^1/_2$	0	0.87/0.13	0.0203(4)/0.0203(4)
S1	4*c*	0	0.2967(3)	$^1/_4$	1.0	0.0142(8)
S2	8*f*	$^1/_2$	0.3573(2)	0.05399(18)	1.0	0.0185(6)
S3	8*f*	1.0	0.5891(2)	0.36313(16)	1.0	0.0139(5)

[a] U_{eq} is defined as one-third of the trace of the orthogonalized U_{ij} tensor.

dx.doi.org/10.1021/ic3018584 | *Inorg. Chem.* 2013, 52, 724−728

Powder X-ray Diffraction (XRD). Powder XRD patterns were taken on handpicked black bar-shaped single crystals at room temperature on a Rigaku DMAX 2500 diffractometer, using monochromatized Cu Kα radiation. Data were collected in the range $2\theta = 10-85°$ with a scan step of 0.05° min^{-1}. The powder XRD pattern is well indexed according to the single-crystal diffraction data shown in Figure 1.

Elemental Analysis. The semiquantitative microprobe elemental analyses of Pb, Mn, In, and S were performed with the aid of a field-emission scanning electron microscope (JSM6700F) equipped with an energy-dispersive X-ray spectrometer (Oxford INCA) on the same single crystals that were used to collect the single-crystal XRD data. The EDX spectroscopy results suggested an empirical formula of $Pb_{0.90(6)}Mn_{0.90(8)}In_2S_{5.2(3)}$, which agreed with the average value revealed by diffraction data of more than 20 crystals from different batches of experiments.

Magnetic Susceptibility. The direct-current magnetic susceptibility measurements were performed on a Quantum Design MPMS-XL magnetometer at a field of 1000 Oe in the temperature range of 2–300 K. The handpicked single crystals were ground to a fine power to minimize possible anisotropic effects and loaded into a gelatin capsule. The data were corrected for the susceptibility of the container and the diamagnetic contribution from the ion core.

UV–Vis Diffuse-Reflectance Spectroscopy. The optical diffuse-reflectance spectrum of $PbMnIn_2S_5$ crystals was measured at room temperature using a Perkin-Elmer Lambda 900 UV–vis spectrophotometer equipped with an integrating sphere attachment and $BaSO_4$ as the reference. The absorption spectrum was calculated from the reflection spectrum via the Kubelka–Munk function: $\alpha/S = (1 - R)^2/2R$, in which α is the absorption coefficient, S is the scattering coefficient, and R is the reflectance.[18]

RESULTS AND DISCUSSION

Crystal Structure. A black bar-shaped crystal with dimensions of about 0.10 × 0.09 × 0.18 mm^3 was mounted on the tip of a glass fiber to collect the diffraction data. $PbMnIn_2S_5$ crystallizes in the $Sr_2Tl_2O_5$ structure type[19] in *Cmcm* (No. 63) with a = 3.896(2) Å, b = 12.731(7) Å, c = 15.770(9) Å, and Z = 1. The structure features a three-dimensional (3D) framework consisting of corrugated layers of condensed $M1S_6$ octahedra (blue in Figure 2) that are interconnected by chains of $M2S_6$ octahedra (green in Figure 2). Also, Pb^{2+} cations occupy the channels within the framework (red in Figure 2). Each $M2S_6$ octahedron propagates into a chain along the a axis by sharing its S2–S2 edge (Figures 2 and 3a). The corrugated layers perpendicular to the b axis (Figure 2) can be regarded as chains of dimeric $M1S_6$ octahedra sharing common S2–S2 edges that are further interconnected at S1 apexes (see the details in Figure 3b).

Note that the M1 (8*f*) and M2 (4*b*) sites are disordered with Mn/In occupancies of 0.43:0.57 and 0.13:0.87, respectively (Table 2). The 43% of Mn substitution is significantly higher than previous reports on Fe substitution in other related compounds, such as 29% in $Pb_{5.5}Fe_{1.5}In_{10}S_{22}$, 9.5% in $Pb_{8.04}Fe_{0.47}In_{17.37}Se_{34}$, or 25% in $Pb_8MIn_{17}S_{34}$ (M = Cu, Ag, Au).[20] We consider that because the ionic radii of In^{3+} and Mn^{2+} are very close, if ordered Mn atoms could be incorporated into Pb–In–Q compounds, unique magnetic properties should be exhibited. Distortion of both MS6 octahedra is indicated by variation of the M–S bond lengths from 2.511(1) to 2.757(2) Å for M1–S and from 2.439(3) to 2.796(2) Å for M2–S (Figure S1 in the SI and Table 3).

The Pb cation is 8-fold-coordinated in a bicapped trigonal prism with Pb–S distances of 3.182(2), 2.755(3), and 3.307(3) Å (Figure S1 in the SI and Table 3). This coordination feature is commonly observed in other related lead chalcogenides.[4–8,19,21–23] Also, distortion of the PbS_8 polyhedron may be related to the stereochemistry activity of Pb^{2+} electrons as

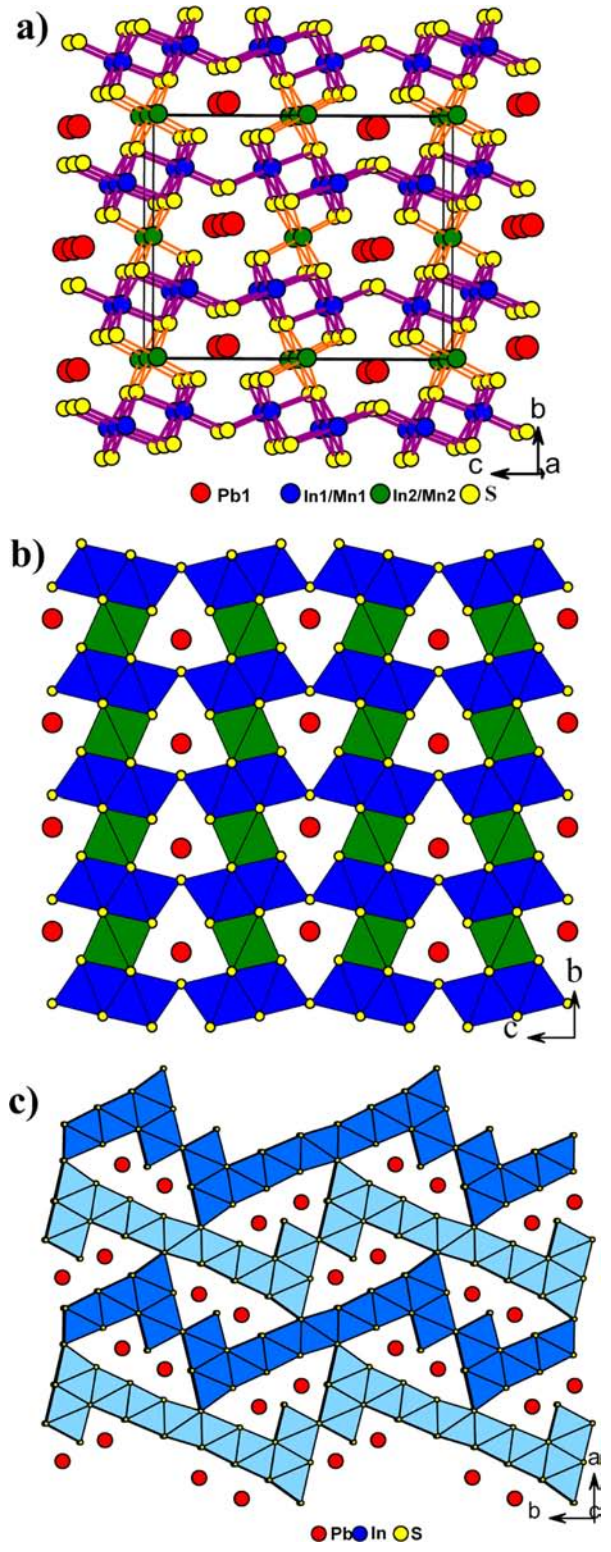

Figure 2. (a) Structure of $PbMnIn_2S_5$ viewed approximately along the a direction with the atom label marked. (b) Polyhedral projection of $PbMnIn_2S_5$ along the a axis. Color code: blue, $(In1/Mn1)S_6$ octahedron; green, $(In2/Mn2)S_6$ octahedron. (c) Polyhedral projection of the related but different $Pb_4In_9S_{17}$[24] along the c axis. Octahedron: InS_6.

dx.doi.org/10.1021/ic3018584 | *Inorg. Chem.* 2013, 52, 724–728

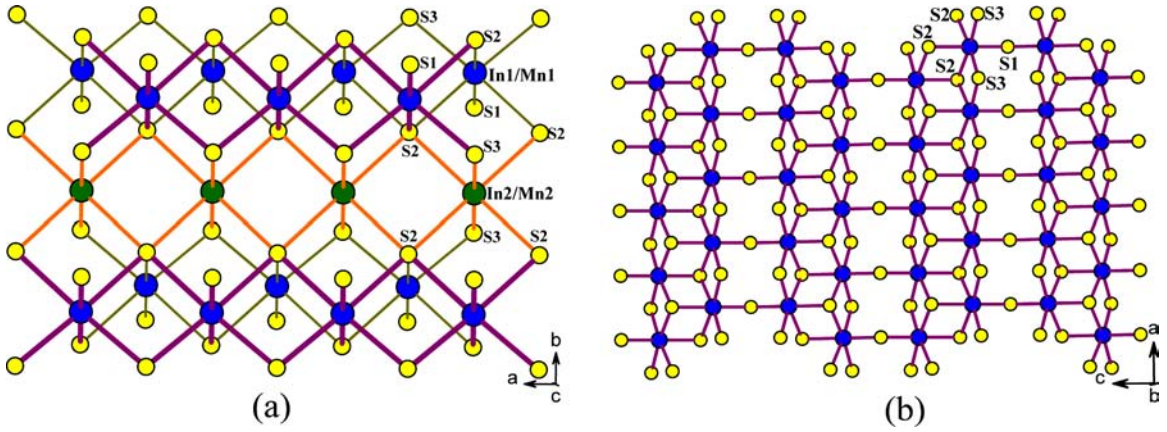

Figure 3. Different structure sections of $PbMnIn_2S_5$: (a) viewed down the *c* axis, chains of dimeric $(In1/Mn1)S_6$ octahedra that are linked by a single chain of $(In2/Mn2)S_6$ octahedra. (b) Corrugated layer of condensed $(In1/Mn1)S_6$ octahedra viewed down the *b* axis. Color code: blue, In1/Mn1; yellow, S.

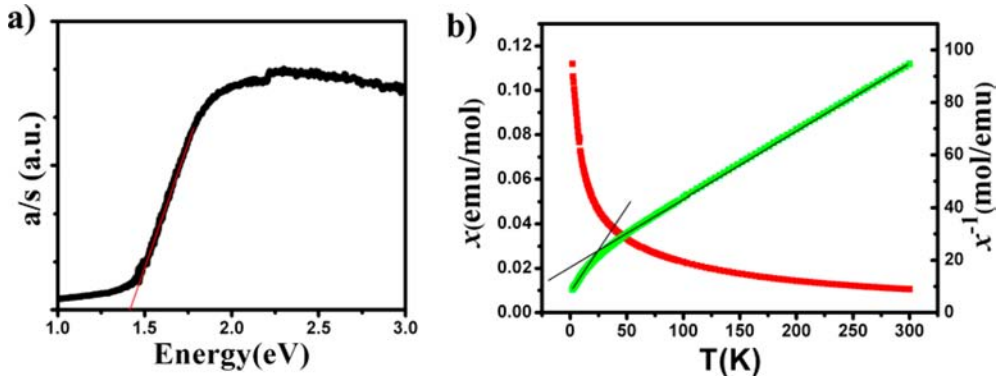

Figure 4. Properties of $PbMnIn_2S_5$: (a) UV−vis diffuse-reflectance spectrum. (b) Temperature (T) dependence of the molar magnetic susceptibility (χ; red line) and the inverse molar magnetic susceptibility (χ^{-1}; green line).

seen in other examples, such as $Pb_{5.5}Fe_{1.5}In_{10}S_{22}$,[6] $Pb_{8.04}Fe_{0.47}In_{17.37}Se_{34}$,[5] and $Pb_8MIn_{17}S_{34}$ (M = Cu, Ag, Au).[20]

Initially, we had considered that Mn substitution of In atoms in $Pb_4In_9S_{17}^{24}$ would generate low-dimensional magnetic chains that should have magnetic properties different from those of the corresponding Pb−Fe−In−S compounds. However, the experimental results reveal that such Mn substitution has totally changed the structure of $Pb_4In_9S_{17}^{24}$ (Figure 2c) into a $Sr_2Tl_2O_5$ structure type,[19] which has never been seen in Pb−M−In (Sb)−Q systems before. Part b versus c in Figure 2 depicts the major difference. Both structures feature 3D frameworks constructed by a MS_6 octahedron with tunnels accommodated by Pb^{2+} cations. The difference comes from the different arrangements of the octahedron unit. In $PbMnIn_2S_5$, the 3D framework looking down the *a* axis can be seen as corrugated layers built by chains of dimeric $[M1S_6]_2$ that are linked by individual $M2S_6$ single chains (Figure 2b). Differently, the 3D network of $Pb_4In_9S_{17}^{24}$ can be viewed as sublayers made by a *Z*-shaped $[InS_6]_9$ nonamer, which are interconnected by common corners (Figure 2c). Such a structure change may come from Mn substitution of In, which splits the *Z*-shaped $[InS_6]_9$ nonamer sublayers into chains of dimeric $[(Mn1/In1)S_6]_2$ and single $(Mn2/In2)S_6$ octahedra. Thus, Mn is important to the formation and stabilization of the title compound. Such a structural role is in accordance with what Fe, Cu, Ag, or Au plays in $Pb_{8.04}Fe_{0.47}In_{17.37}Se_{34}$,[5] $Pb_{5.5}Fe_{1.5}In_{10}S_{22}$,[6] or $Pb_8MIn_{17}S_{34}$ (M = Cu, Ag, Au).[20] Besides, the disorder manner of Mn/In in the title compound is similar to those in $Pb_{5.5}Fe_{1.5}In_{10}S_{22}$[6] and $Pb_{8.04}Fe_{0.47}In_{17.37}Se_{34}$.[5]

Optical Properties. The optical diffuse-reflectance spectrum measured on handpicked crystals of $PbMnIn_2S_5$ at room temperature suggests an optical band gap of 1.45 eV (Figure 4a), which is consistent with its black color. This value is larger than those of $Pb_{5.5}Fe_{1.5}In_{10}S_{22}$ (0.95 eV) and $Pb_8MIn_{17}S_{34}$ (M = Cu, Ag, Au) (about 1.3 eV).[6,20]

Magnetic Properties. The molar magnetic susceptibility of $PbMnIn_2S_5$ was measured at an applied field of 1000 Oe in the temperature range of 2−300 K (Figure 4b). The magnetic susceptibility obeys the Curie−Weiss law above 40 K and deviates below 40 K. Also, a least-squares method fit was implemented at the temperature dependence of the inverse molar magnetic susceptibility from 40 to 300 K with the Curie−Weiss equation $\chi_M = C/(T - \theta)$, where χ_M is the magnetic susceptibility, C the Curie constant, and θ the Weiss constant. As a result, C = 3.84 emu K mol^{-1} and θ = −66.61 K were obtained. The observed effective magnetic moment, $\mu_{eff} \approx$ 5.54 μ_B, calculated from the equation $\mu_{eff} = (7.997C)^{1/2}\mu_B$,[25] agrees with the calculated μ_{eff} = 5.92 μ_B according to the equation $\mu_{eff}(total) = \mu_{eff}(Mn^{2+})$.[26] The calculated μ_{eff} is slightly higher than the observed one, suggesting that Mn^{2+} cations are in the high-spin state ($t_{2g}^3e_g^2$; S = 2.5). The negative θ suggests significant antiferromagnetic interactions between Mn^{2+} cations (the nearest Mn−Mn distance is 3.762 Å). In comparison, both $PbMnIn_2S_5$ and $Pb_4MnSb_6S_{14}$, a related but totally different

dx.doi.org/10.1021/ic3018584 | Inorg. Chem. 2013, 52, 724−728

compound,[21] exhibit antiferromagnetic interactions between Mn^{2+} anions in the high-spin state with similar μ_{eff}, 5.54 versus 5.7 μ_B.[21] Such observed effective magnetic moments are lower than the calculated value, which may be ascribed to the covalency effects.[27]

CONCLUSION

In summary, the first manganese member in the Pb−M−In−S system, $PbMnIn_2S_5$, has been discovered, which adopts the $Sr_2Tl_2O_5$ structure type,[19] which has never been seen in such systems before. The two crystallographically distinguished octahedral sites are disordered by Mn and In with occupancies of 0.43:0.57 and 0.13:0.87. The optical band gap is estimated to be 1.45 eV, consistent with its black color, and antiferromagnetic interactions obeying the Curie−Weiss law above 40 K are observed between high-spin Mn^{2+} cations ($t_{2g}^3e_g^2$; $S = 2.5$). The Pb−M−In (Sb)−Q compounds with ordered Mn atoms, which should exhibit unique interesting magnetic properties, are under exploration.

ASSOCIATED CONTENT

Supporting Information

CIF data, EDS data, and the formulas and occupied ratios of five single crystals. This material is available free of charge via the Internet at http://pubs.acs.org.

AUTHOR INFORMATION

Corresponding Author

*E-mail: chenl@fjirsm.ac.cn. Tel: (011)86-591-83704947.

Notes

The authors declare no competing financial interest.

ACKNOWLEDGMENTS

This research was supported by the National Natural Science Foundation of China under Projects 90922021, 20973175, and 21171168 and the "Knowledge Innovation Program of the Chinese Academy of Sciences" (Grant KJCX2-YW-H20).

REFERENCES

(1) Wintenberger, M.; Andre, G. *Physica B* **1990**, *162*, 5−12.
(2) Leone, P.; Andre, G.; Doussier, C.; Moelo, Y. *J. Magn. Magn. Mater.* **2004**, *284*, 92−96.
(3) Leone, P.; Doussier-Brochard, C.; Andre, G.; Moelo, Y. *Phys. Chem. Miner.* **2008**, *35*, 201−206.
(4) Matsushita, Y.; Ueda, Y. *Inorg. Chem.* **2003**, *42*, 7830−7838.
(5) Matsushita, Y.; Sugiyama, K.; Ueda, Y. *Inorg. Chem.* **2006**, *45*, 6598−6600.
(6) Matsushita, Y.; Ueda, Y. *Inorg. Chem.* **2006**, *45*, 2022−2026.
(7) Showron, A.; Brown, I. D. *Acta Crystallogr.* **1990**, *C46*, 2287−2291.
(8) Poudeu, P. F. P.; Takas, N.; Anglin, C.; Eastwood, J.; Rivera, A. *J. Am. Chem. Soc.* **2010**, *132*, 5751−5760.
(9) Makovicky, E.; Karup-Mollar, S. *Neues Jahrb. Mineral., Abh.* **1977**, *130*, 264−287.
(10) Gostojic, M.; Nowacki, W.; Engel, P. *Z. Kristallogr.* **1982**, *159*, 217−224.
(11) Park, Y. B.; Choi, D. S. *Bull. Korean Chem. Soc.* **2004**, *25*, 1095−1097.
(12) Chondroudis, K.; Kanatzidis, M. G. *J. Solid State Chem.* **1998**, *136*, 328−332.
(13) McCarthy, T. J.; Tanzer, T. A.; Kanatzidis, M. G. *J. Am. Chem. Soc.* **1995**, *117*, 1294−1301.
(14) Iordanidis, L.; Bilc, D.; Mahanti, S. D.; Kanatzidis, M. G. *J. Am. Chem. Soc.* **2003**, *125*, 13741−13752.
(15) Sheldrick, G. M. *SADABS*, University of Göttingen: Göttingen, Germany, 1996.
(16) *CrystalClear*, version 1.3.5; Rigaku Corp.: The Woodlands, TX, 1999.
(17) Sheldrick, G. M. *SHELXTL, Crystallographic Software Package*, version 5.1; Bruker AXS: Madison, WI, 1998.
(18) Kortüm, G. *Reflectance Spectroscopy*; Springer-Verlag: New York, 1969.
(19) Berastegui, P.; Eriksson, S.; Hull, S.; Garcia Garcia, F. J.; Eriksen, J. *Solid State Sci.* **2004**, *6*, 433−441.
(20) Wang, K. C.; Lee, C. S. *Inorg. Chem.* **2006**, *45*, 1415−1417.
(21) Leone, P.; Le Leuch, L. M.; Palvadeau, P.; Molinie, P.; Moelo, Y. *Solid State Sci.* **2003**, *5*, 771−776.
(22) Iordanidis, L.; Kanatzidis, M. G. *Inorg. Chem.* **2001**, *40*, 1878−1887.
(23) Kramer, V. *Acta Crystallogr., Sect. C* **1983**, *39*, 1328−1329.
(24) Ginderow, D. *Acta Crystallogr., Sect. B* **1978**, *34*, 1804−1811.
(25) O'Connor, C. J. *Prog. Inorg. Chem.* **1982**, *29*, 209−283.
(26) West, A. R. *Solid State Chemistry and Its Applications*; John Wiley & Sons: Chichester, U.K., 1984.
(27) Burlet, P.; Ressouche, E.; Malaman, B.; Welter, R.; Sanchez, J. P.; Vulliet, P. *Phys. Rev. B* **1997**, *56*, 14013−14018.